A Numerical Optimization Framework for Rotor Airfoil Design
48th European Rotorcraft Forum, 6. September 2022, Winterthur, CH

Gunther Wilke
Institute of Aerodynamics and Flow Technology

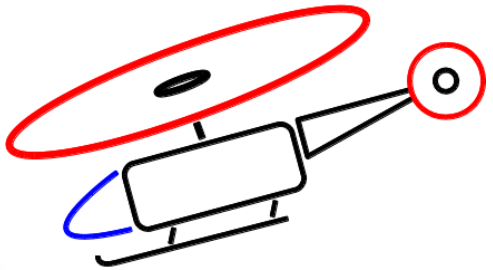

DLR

Introduction & Motivation

- Airfoil design is still often done manually with many constraints to be obeyed and multiple flow conditions to be considered

- Direct numerical optimization of the rotor for design conditions allows to find new airfoils also, but cannot guarantee success in off-design conditions

- Novelties over existing approaches are:
  - Surrogate based optimization for multiple goal functions is carried out
  - Each goal function is made up of a mean value for a range of lift coefficients
  - The selected airfoils are validated against full rotor simulations

- The chosen rotor to be optimized is the HART II rotor
  - Public data available
  - NACA 23012 is a well known airfoil
  - Also attempt of an airfoil family with 9% airfoil at tip (NACA 23009 as starting point)
  - Comparison against more recent OA212/OA209 airfoils

Overview

- Introduction & Motivation
- Methodology & Validation
- Optimization Results
- Verification of Rotor Design Gains
- Conclusions

Methodology: Optimization Strategy & Parameterization

- The optimization is done using a surrogate based optimization technique, Wilke [34]
  - Kriging Surrogate model used
  - ‘crashmap’ technique to avoid penalty function
  - Multi-objective optimization technique to concurrently optimized airfoils for multiple flow conditions

- For the parameterization, the improved geometric parameterization (IGP) by Xiaoqiang et al. [11] is used with modifications
  - Approach describes camberline and (generalized NACA) thickness distribution of the airfoil
  - Camberline here described with 5 NURBS points (4 parameters)
  - Noise radius, location of max. thickness & boat angle are set free
  - Additionally a tap function is applied, where the tab angle is set free
    → total of 8 design variables set by the optimizer

Airfoil comparison of NACA 23012 with IGP fit

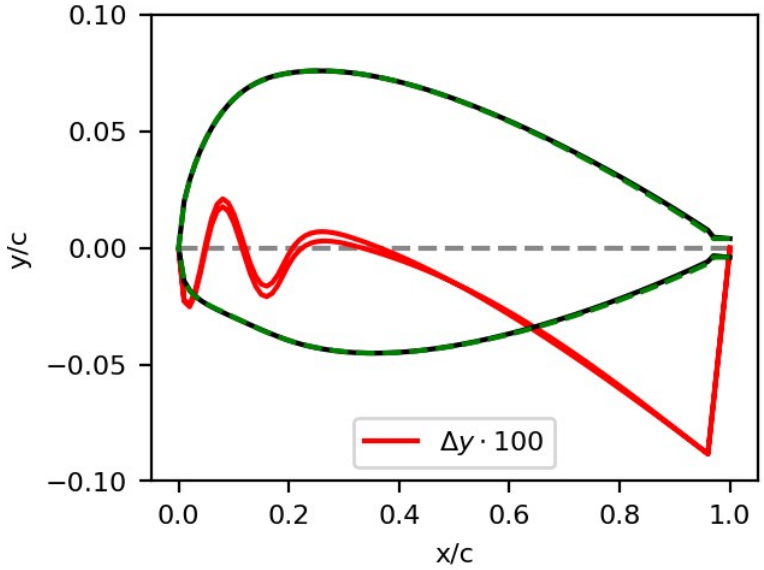

camberline and thickness distribution of IGP fit

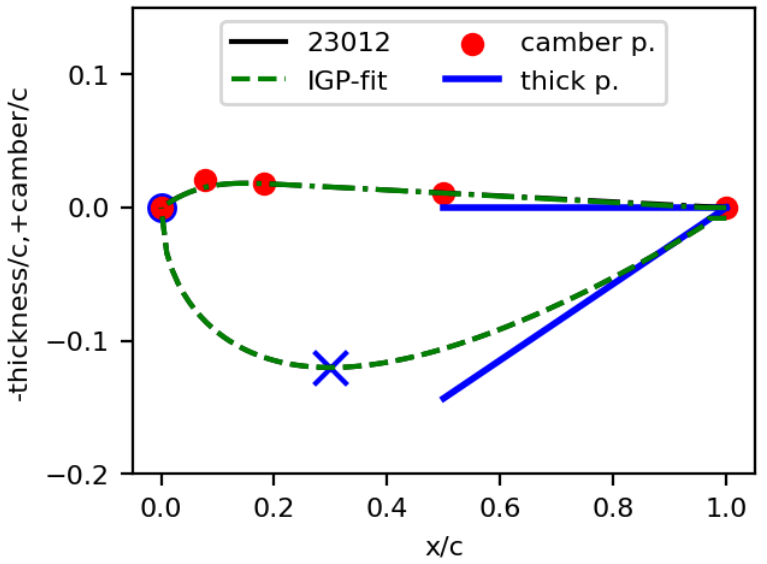

Methodology: Simulation & Validation

- DLR's FLOWer block-structured CFD solver [40] used for airfoil simulations
  - 3rd order MUSCL [43,44] with SLAU2 [42] upwind scheme used
  - SA turbulence model [45]
  - Emperical Transition prediction
    - Tollmien-Schlichting through AHD [46] or p_{min} in case of shocks
    - Laminar separation
  - Steady simulation through local time stepping with LU-SGS [49]

- Validation against DSA-9A airfoil case from Richter et al. [37]

- 192x96 cells used during optimization

inviscid drag only!

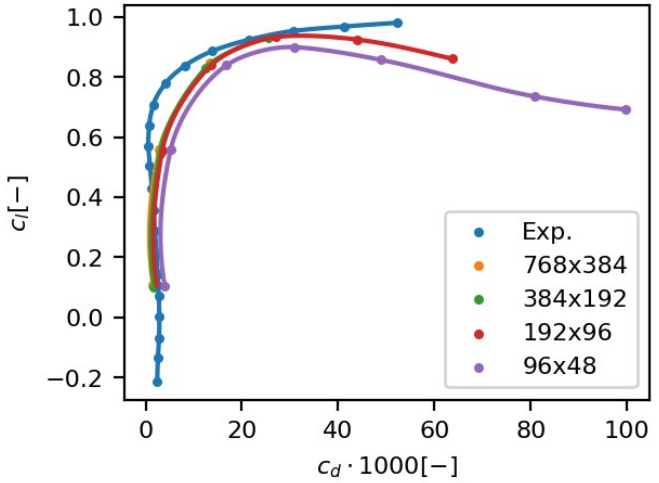

Mach 0.6

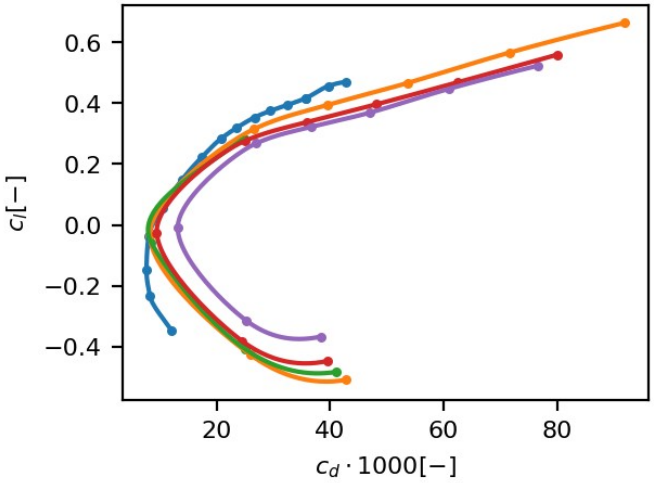

Mach 0.85

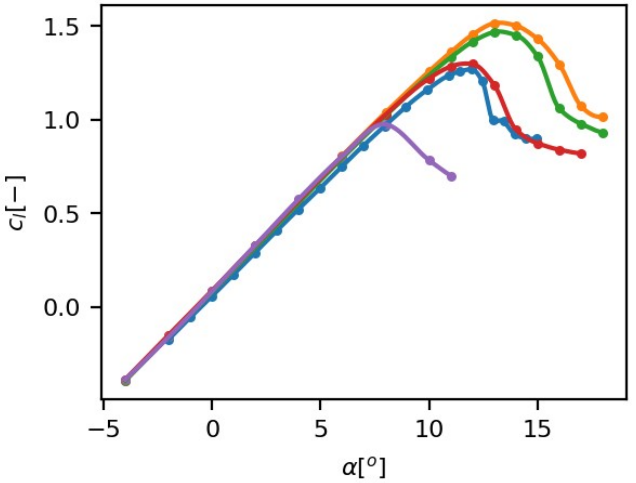

Mach 0.3

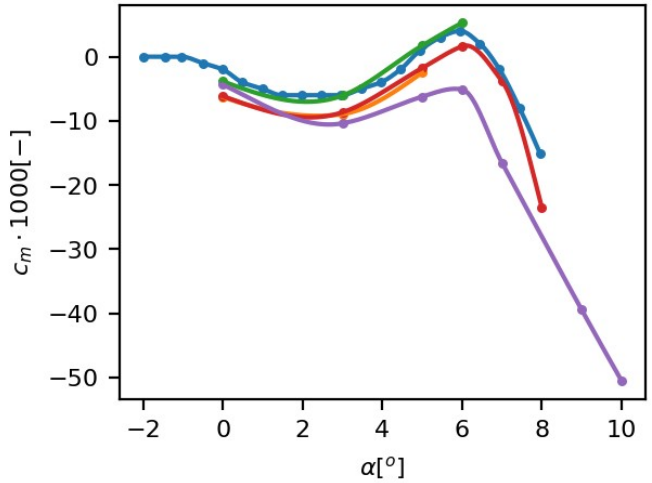

Mach 0.6

Methodology: Simulation & Validation

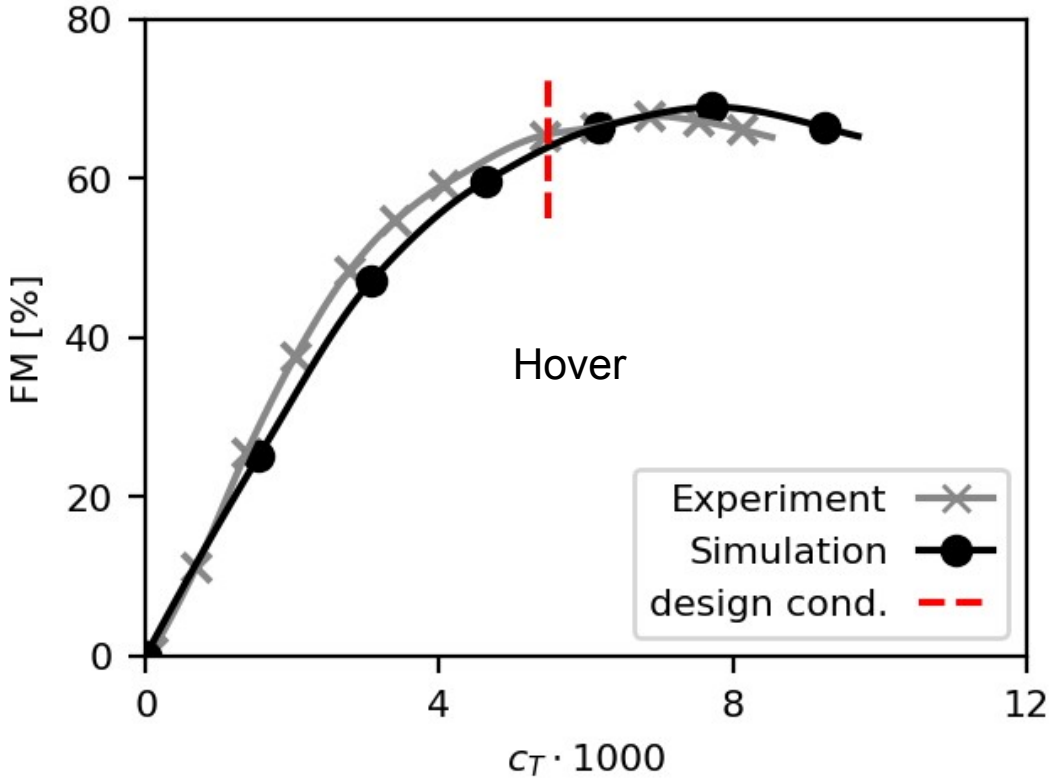

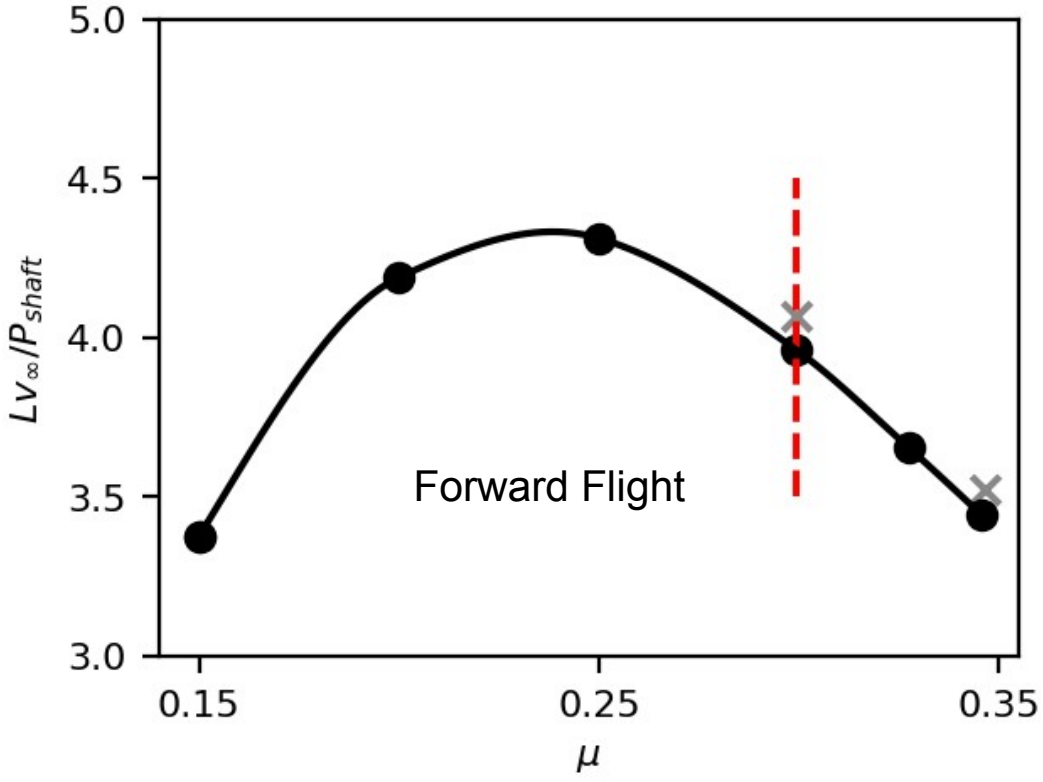

- The airfoils are also validated through rotor simulations. They themselves have been validated against the results of the Bo105 blade (aka HART II) used during the FTK wind tunnel campaign [39].
- The simulations are fluid-structured coupled (FLOWer + HOST [52]) and trimmed. In hover a periodic mesh is used, in forward flight a Chimera setup with all 4 blades and the fuselage is modeled. MUSCL extrapolation of 4th order, SA-DDES-R as turbulence model. 670,000 grid cells in hover, 2.2e6 cells in forward flight.

Optimization: Flight condition estimation

- Selected two flight conditions from FTK wind tunnel campaign [39] to improve the HART II blade

- Applied to estimations for the required lift coefficient
  - 6 C_T / σ
  - Inversely formulated BEMT

$$c_l = c_z cos\phi - c_x sin\phi \quad (1)$$

$$\phi = arctan(v_i/V) \quad (2)$$

$$v_i \approx -\frac{v_\infty sin\alpha_q}{2} \pm \sqrt{|(\frac{v_\infty sin\alpha_q}{2})^2 + \frac{n_{blades} dF_z}{4\Pi\rho_\infty r dr}|} \quad (3)$$

$$V \approx \Omega r + v_\infty sin\psi \quad (4)$$

- It becomes apparent that rotor airfoils need to be optimized for a wide range of lift coefficients

  - Especially the tip airfoil is challenging:
    - High lift coefficients in hover
    - Transonic conditions on advancing side with zero-lift coefficient

Hover lift coefficient estimation

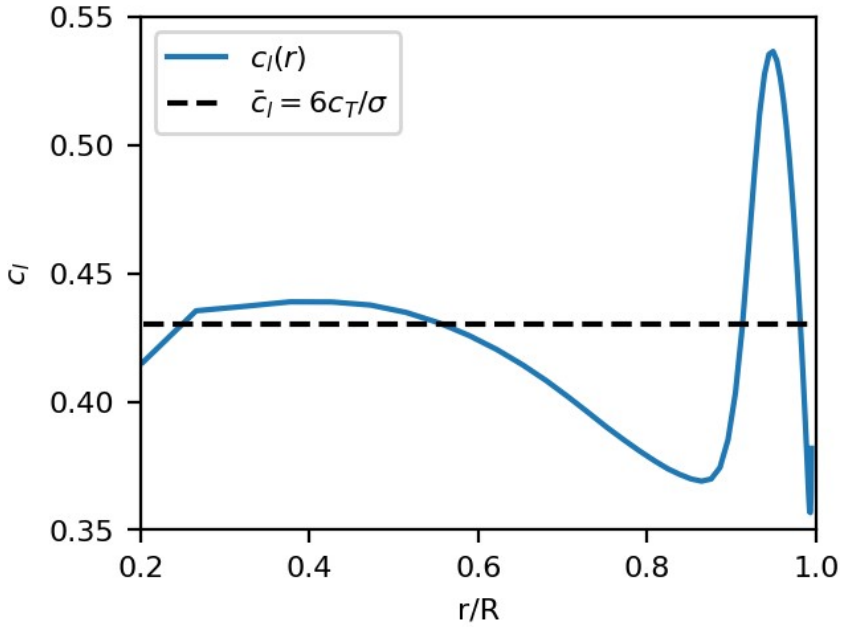

Forward flight lift coefficient estimation (μ=0.3)

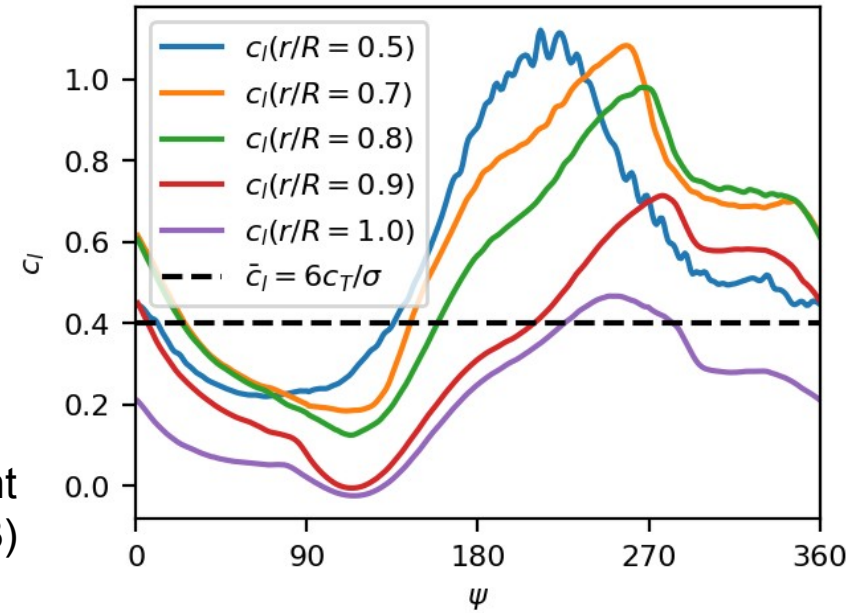

Optimization: Goal function setup

Optimization of 3 different airfoils

12% only	Mach	Re x 10^6	c_l range
retreating	0.10	0.1	max
hover	0.65	1.9	0.2 ... 0.6
advancing	0.75	2.1	-0.2 ... 0.2
12% inboard	Mach	Re x 10^6	c_l range
retreating	0.10	0.1	max
hover	0.52	1.5	0.3 ... 0.6
advancing	0.75	2.1	-0.1 ... 0.3
9% outboard	Mach	Re x 10^6	c_l range
retreating	0.42	1.2	max
hover	0.65	1.9	0.2 ... 0.4
advancing	0.88	2.5	-0.2 ... 0.1

Table of flow conditions

- Goal functions are the minimization of drag in a) hover and b) advancing side flow conditions
- Constraints are maximum lift in the retreating side condition and pitching moment in hover

- Computation of airfoil polars at the select Mach numbers (32 data points per airfoil)
- Extraction of numbers for the given c_l range
  - Use of modified Akima splines for interpolation [5]
  - 2nd order polynomial for maximum lift coefficient

Extraction of mean drag coefficient

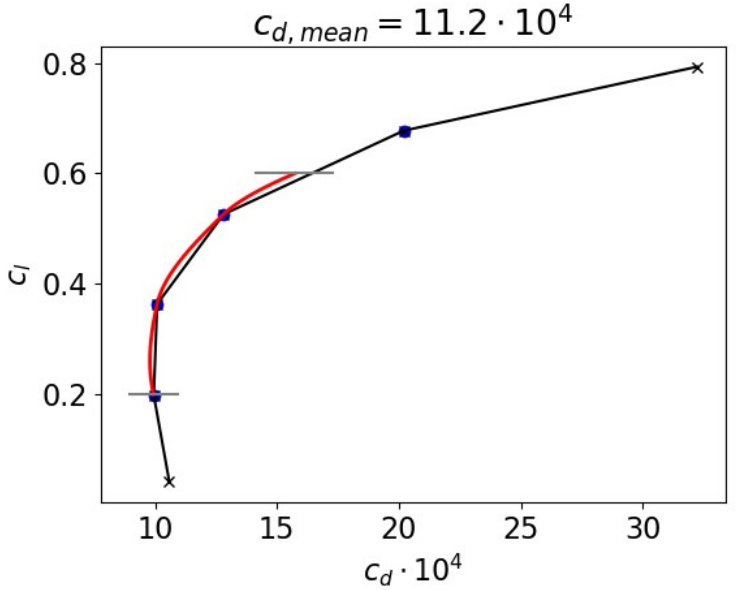

Extraction of maximum lift coefficient

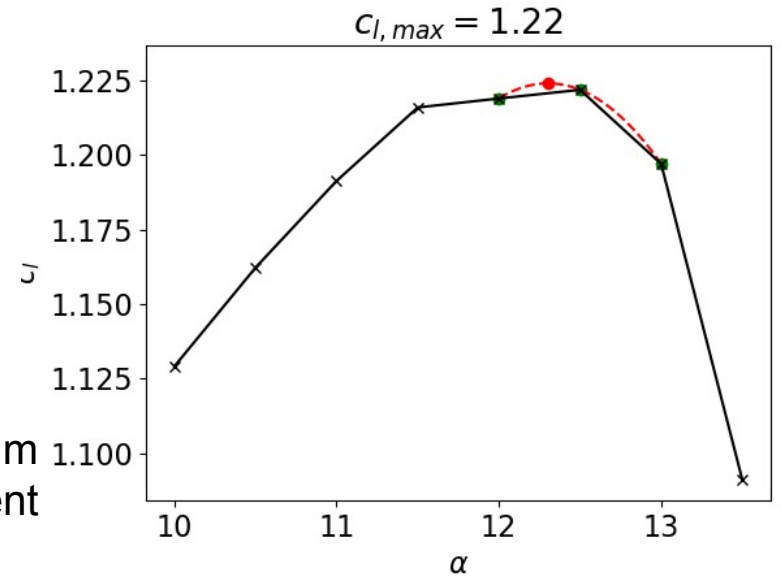

Optimization Results: Pareto Fronts

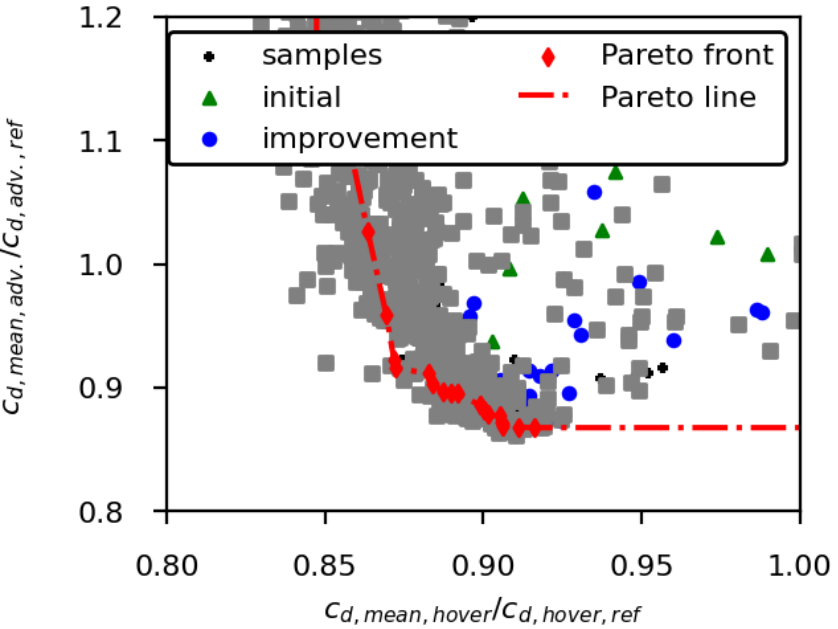

12% airfoil only optimization

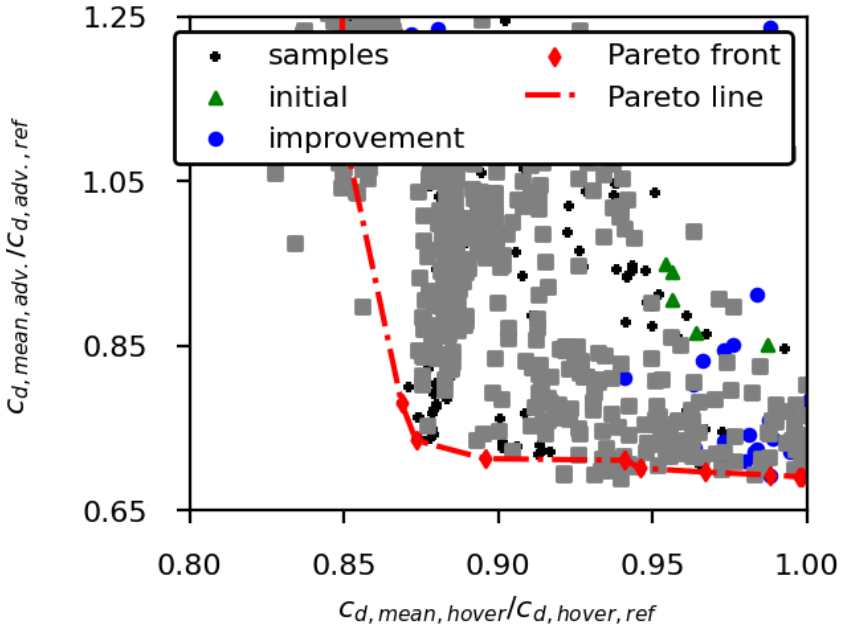

12% inboard optimization

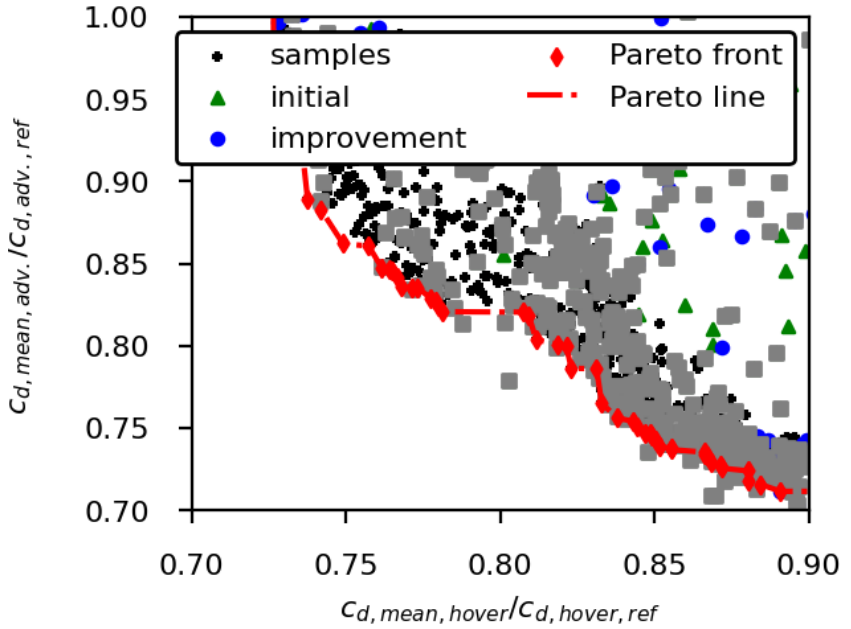

9% outboard optimization

- Optimizations used somewhere between 1120 and 1368 simulations. A large quantity violates the constraints (42-85%).
- The next slides show a selection of airfoils. The best in each goal function that maintained a similar performance in the opposing goal function as the reference airfoil.

Optimization Results: 12% only - geometry

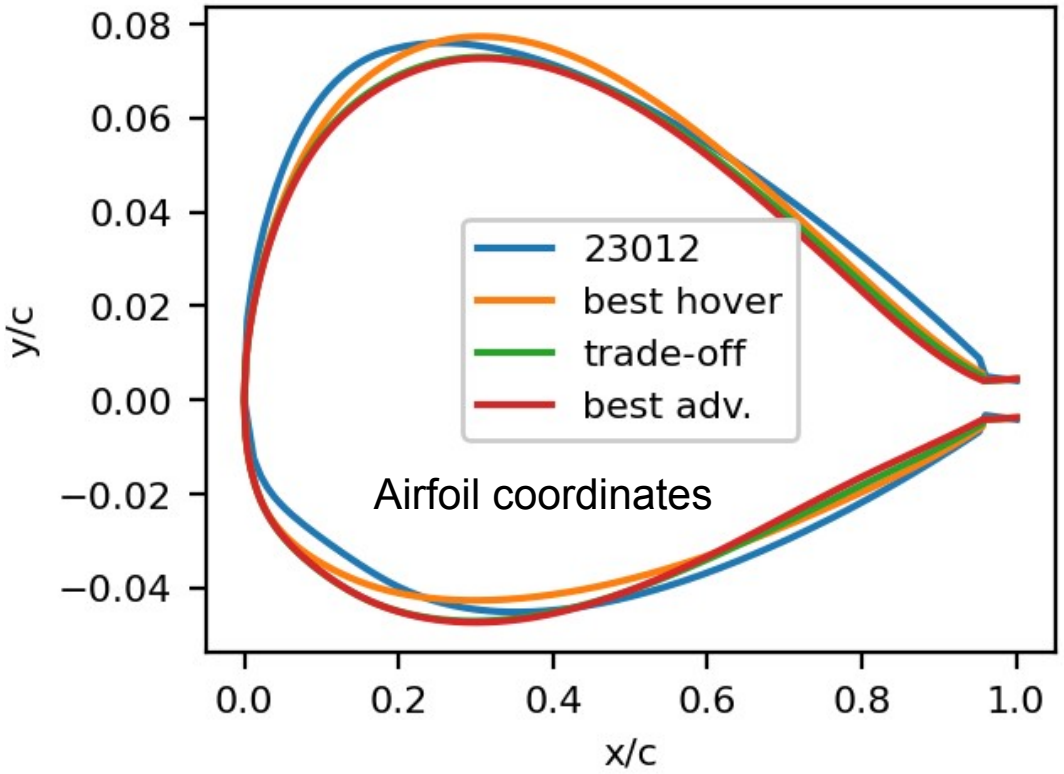

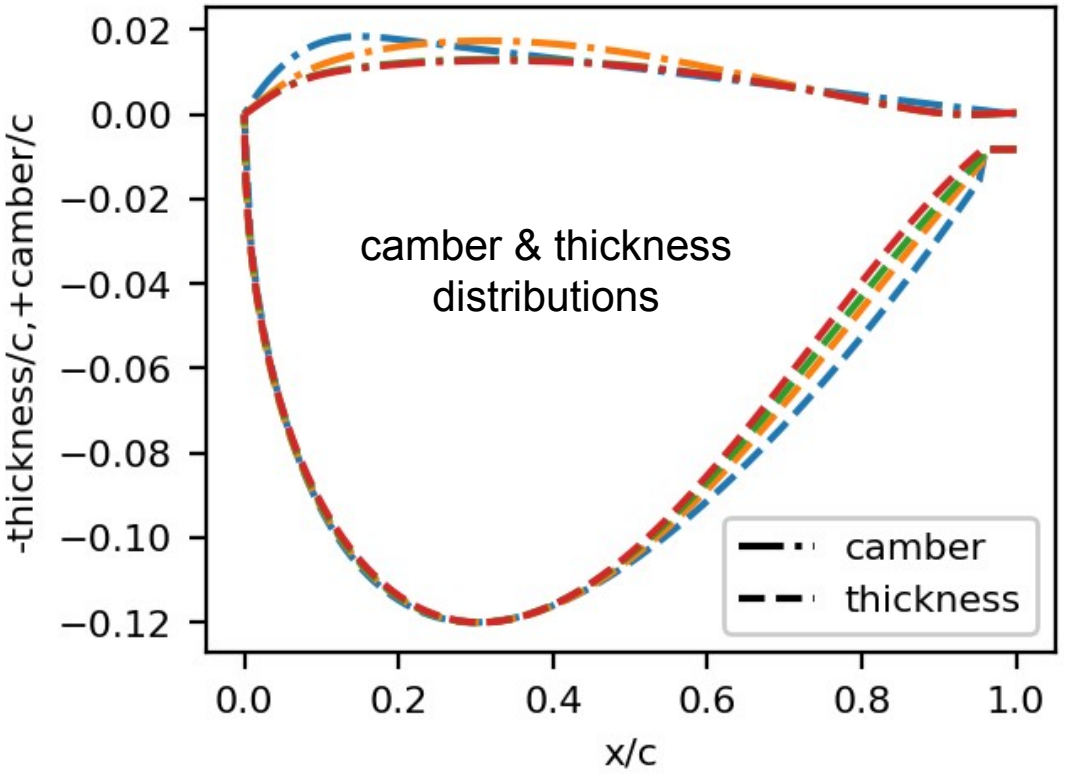

- The location of maximum thickness remains at x/c=30% with a very mild reduction in nose radius (from 2% to 1.7% for best hover)
- Maximum camber reduced from 1.8% to 1.3% for the the trade-off and best adv. airfoil. Location of max. camber further aft at 31-33% vs 15% for NACA 23012

Optimization Results: 12% only - polars

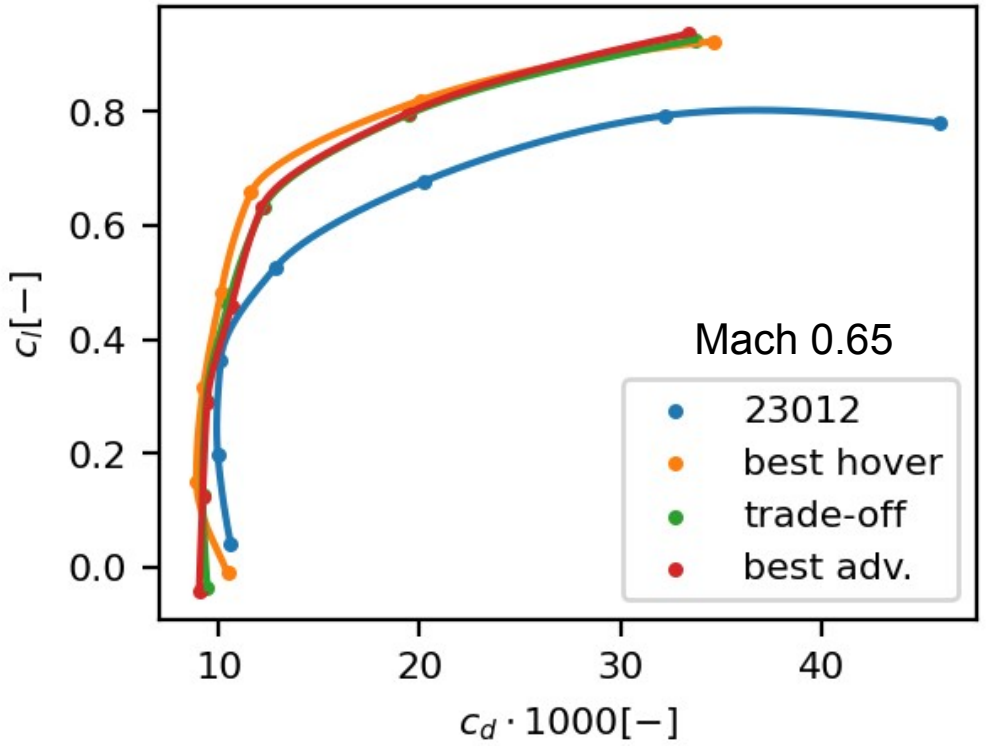

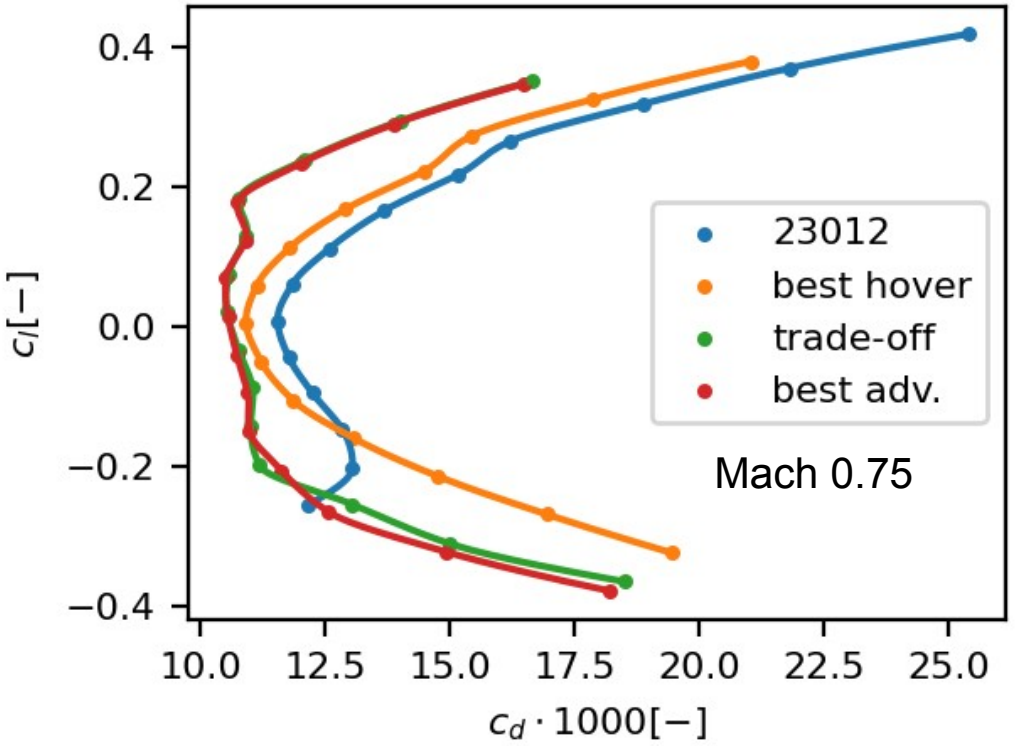

- All airfoils improve over the NACA23012 in both flight conditions
- The hover biased airfoil improves at higher lift coefficients in hover, but sacrifices drag at lower lift coefficients (out of the optimization range) and only mildly improves at the adv. side flow condition.
- The trade-off design has been chosen close to the best adv. design. It sacrifices less performance in hover than the best adv. design

Optimization Results: 12% only – pressure distributions @ mean c_l

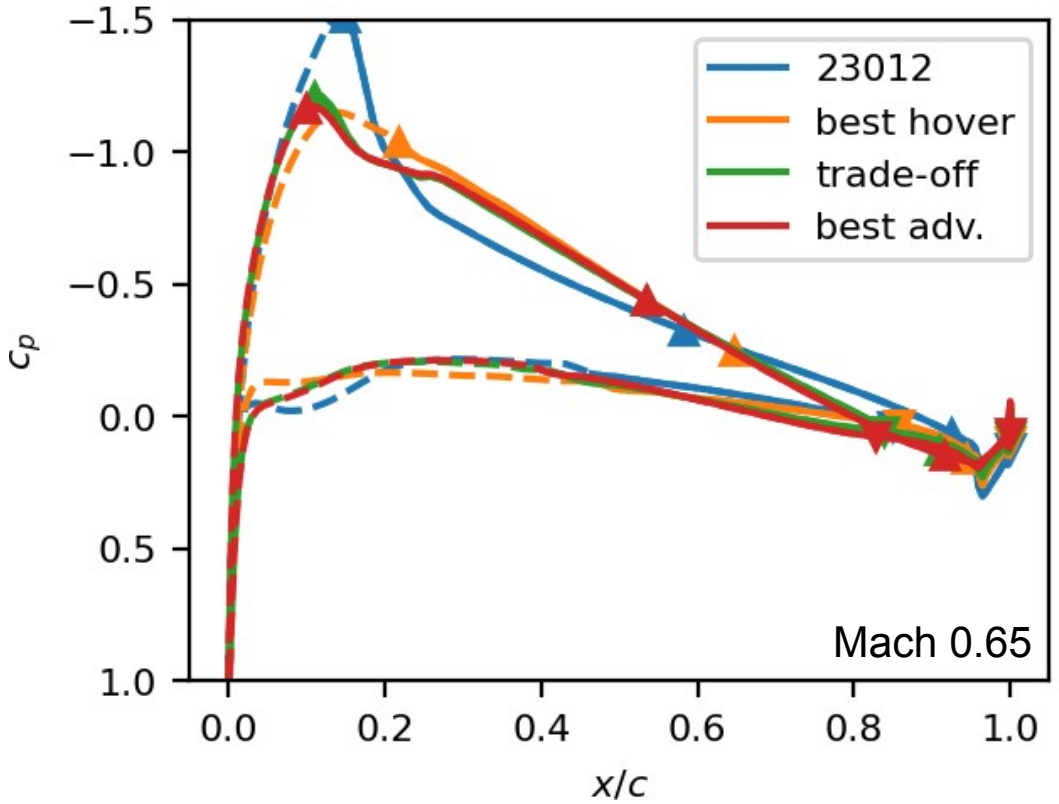

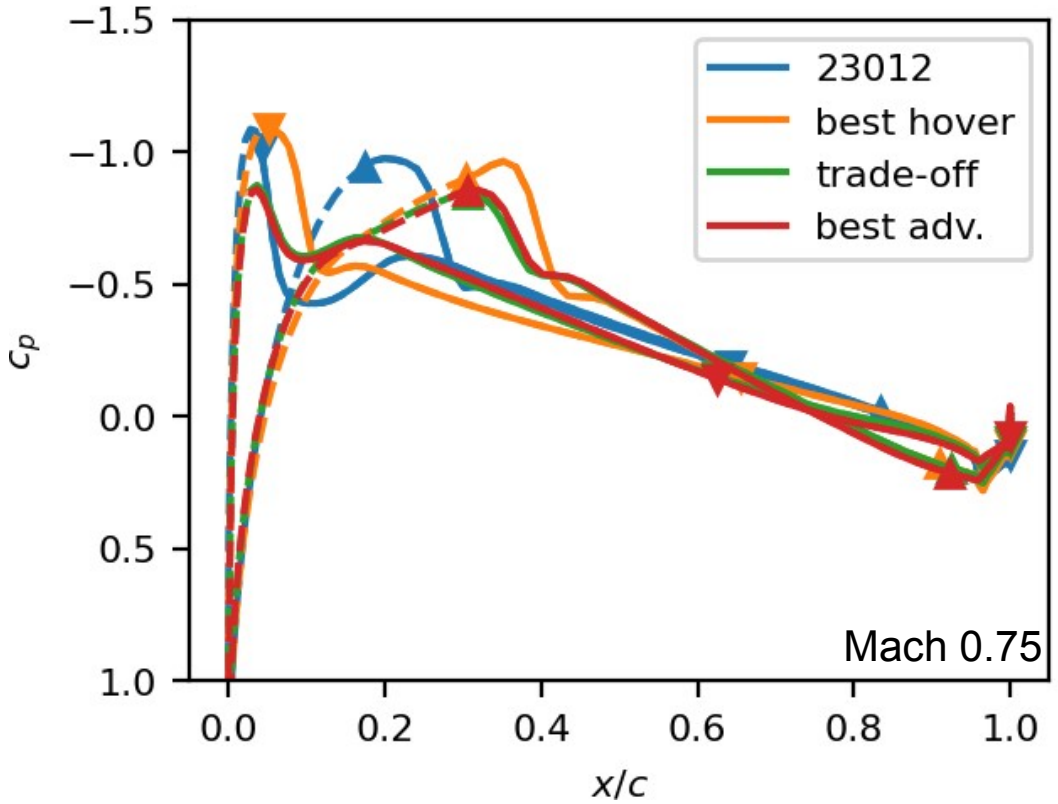

- Dashed lines indicate laminar flow regions
- The hover design shows a smoother suction peak in hover, whereas a stronger shock is found for the adv. side flow condition.
- The trade-off airfoil is very similar to the best adv. design, but has a slightly better pressure side in hover over the best adv. side design.

Optimization Results: 12% inboard - geometry

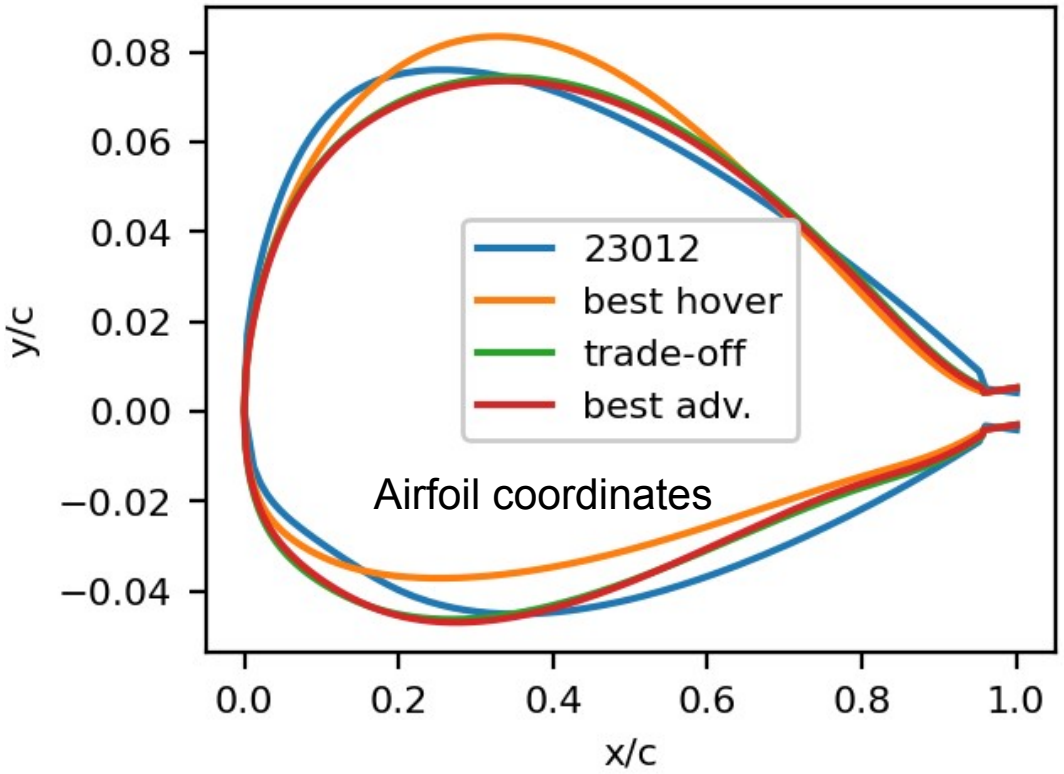

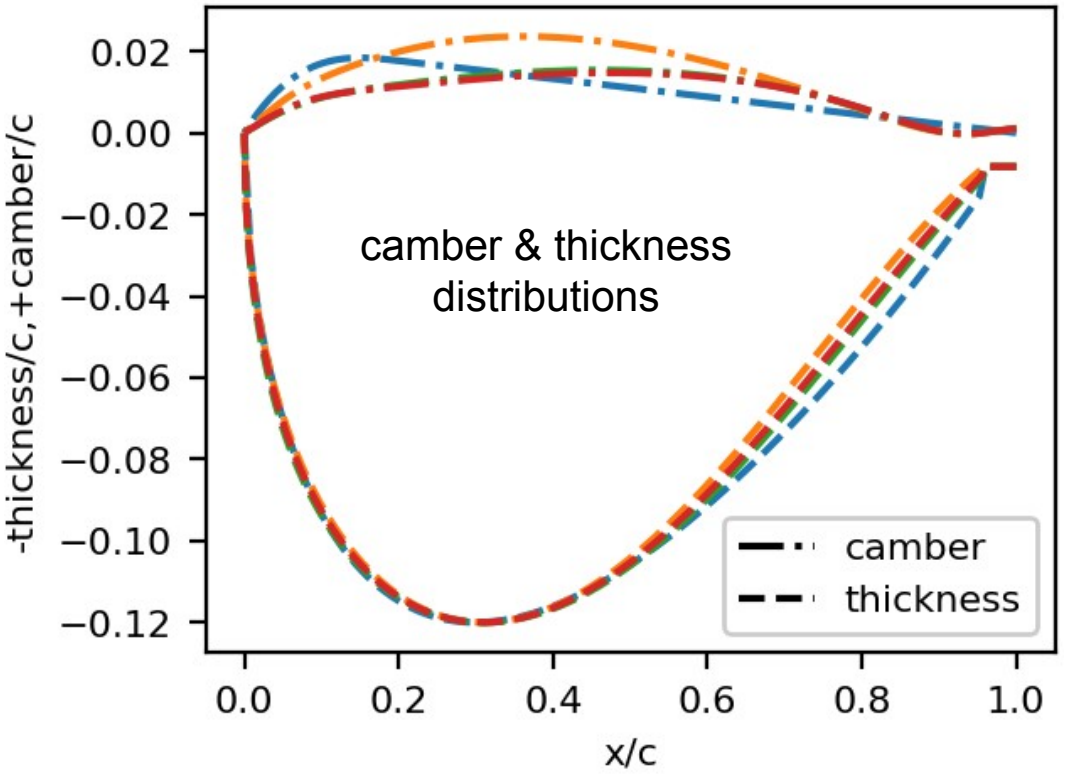

- The location of maximum thickness shifted slightly towards x/c=31% with a very mild reduction in nose radius (from 2% to 1.6% for best hover)
- Maximum camber noticeable increased from 1.8% to 2.4% for the hover airfoil, the trade-off and best adv. Airfoils have 1.5%
- General camber shape quit different, more aft, delays flow acceleration in advancing side condition.

Optimization Results: 12% inboard - polars

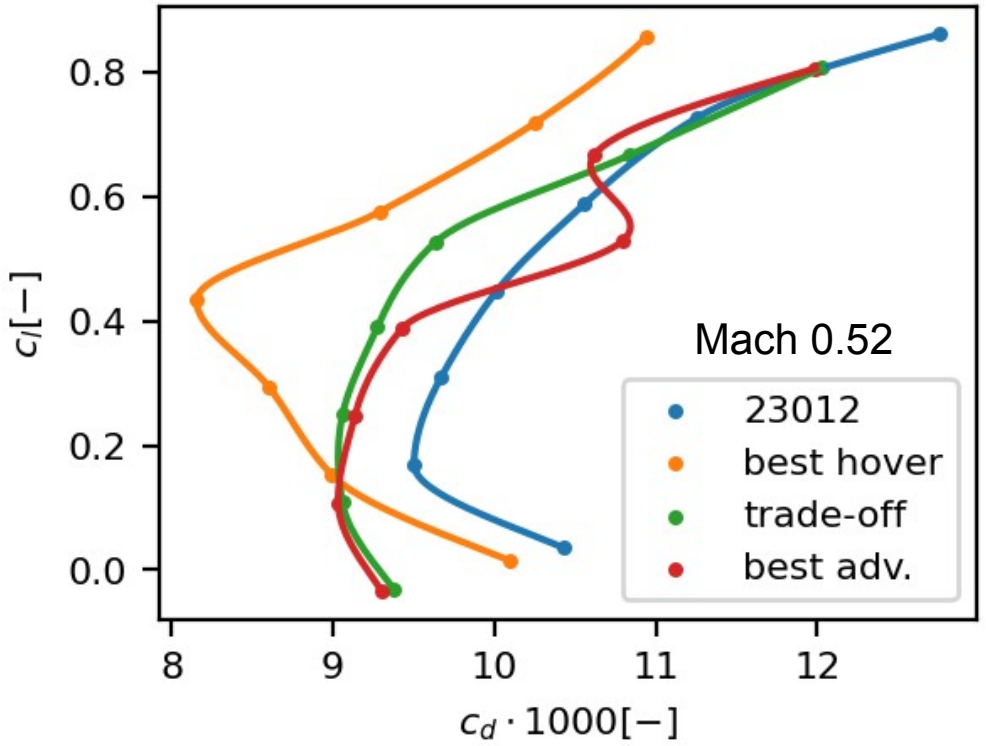

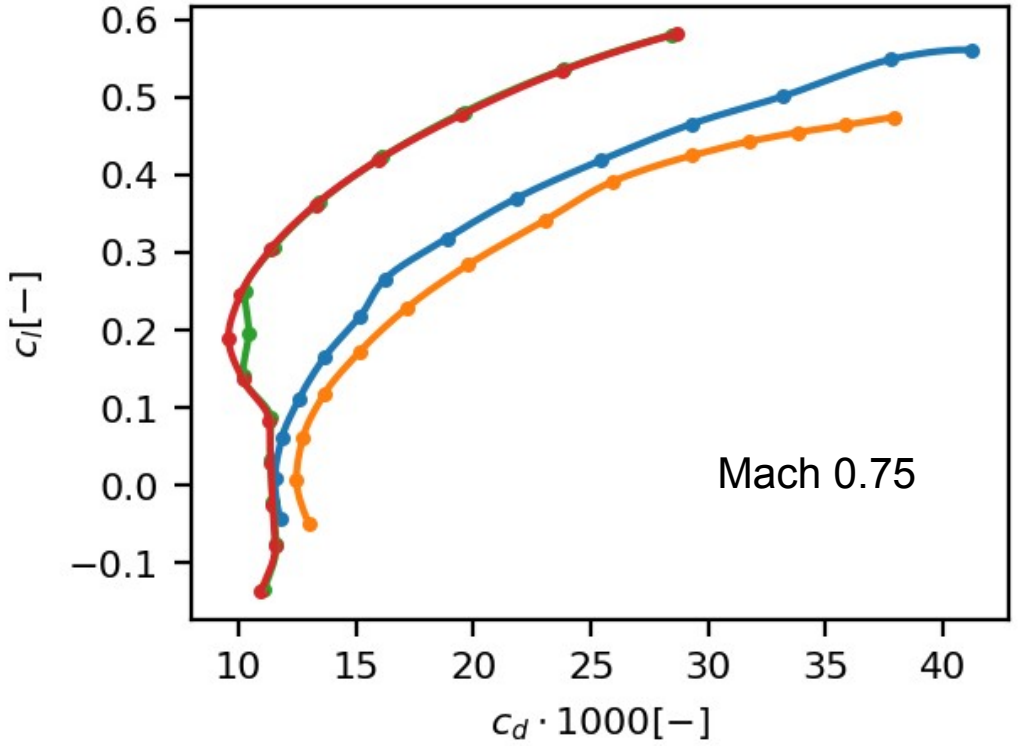

- The 12% inboard optimization shows the trade-offs from the optimization: the best hover airfoil reduces the drag significantly in the hover condition and is slightly worse in the advancing side condition
- The best advancing side design improves in both goal functions
- Therefore, a trade-off close to the advancing design was selected, improving at higher lift coefficients in hover without significantly loosing performance in the advancing side condition

Optimization Results: 12% inboard – pressure distributions @ mean c_l

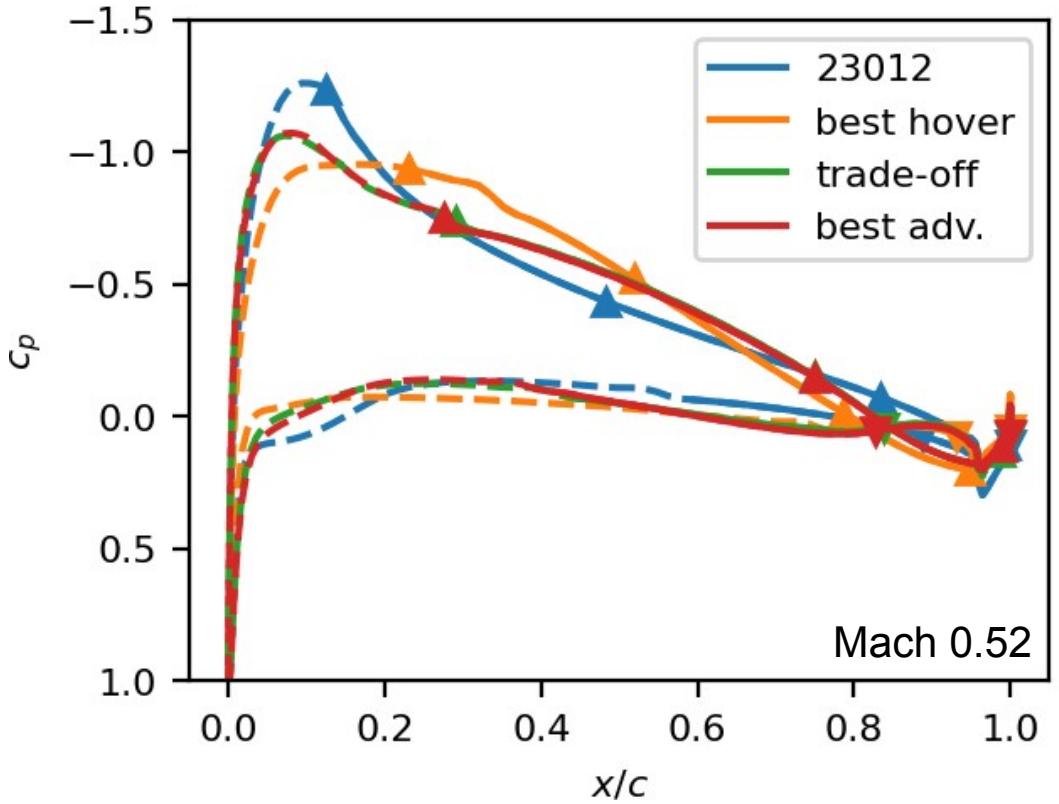

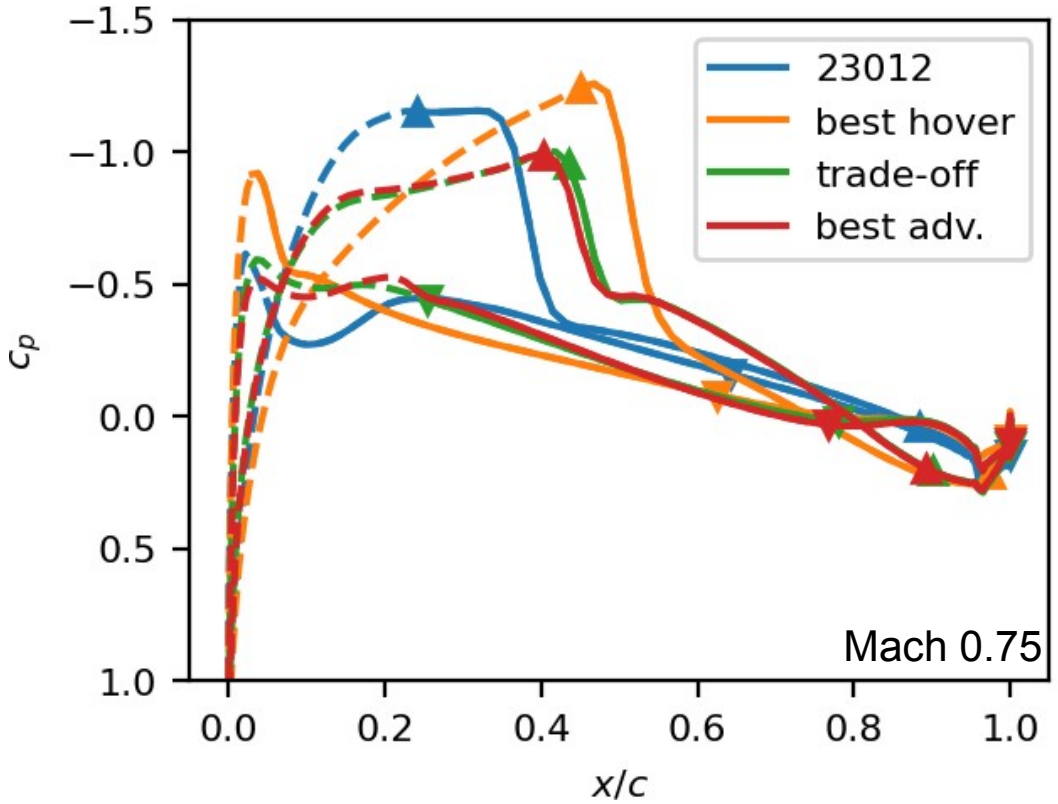

- The delayed but larger camber of the best hover airfoils leads to a very good pressure distribution in hover, but the shock becomes more severe in the adv. side flow condition, which is partially compensated by a greater laminar area (dashed lines)
- The best adv. airfoil and trade-off airfoil are close together in the pressure distribution, yet a longer laminar area on the pressure side reduce the overall drag.

Optimization Results: 9% outboard - geometry

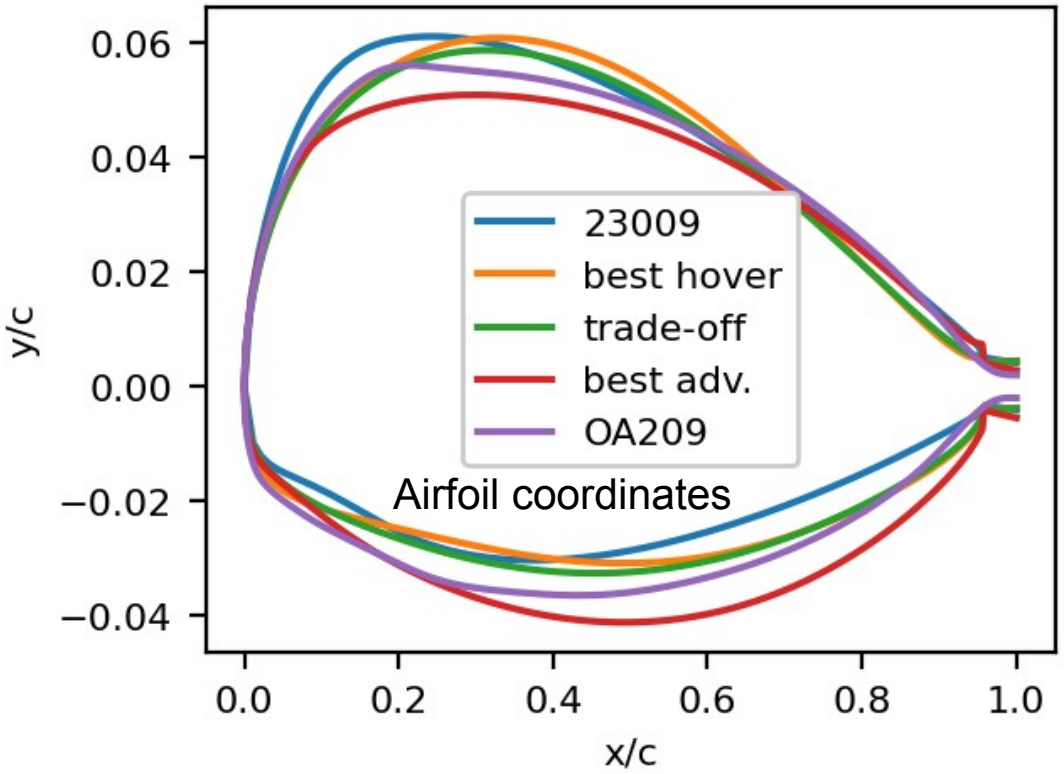

camber & thickness distributions

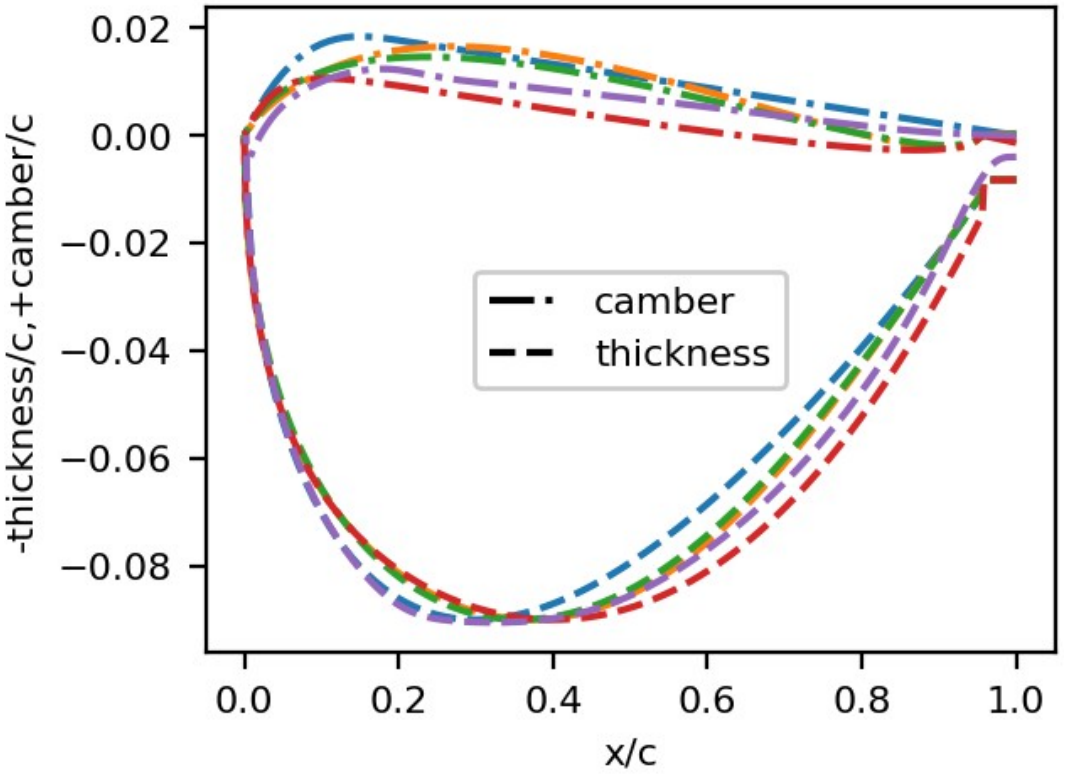

- The range of the location of maximum thickness varies more than for the inboard optimization 36% for the trade-off vs 40% for the best adv. airfoil. Nose radius very similar between 1.0 ...1.1%
- Location of and max. camber varies from (27%,1.7%) (hover airfoil) to (11%,1.1%) (best adv. airfoil)
- A much larger diversity and therefore the trade-off was carefully selected

Optimization Results: 9% outboard - polars

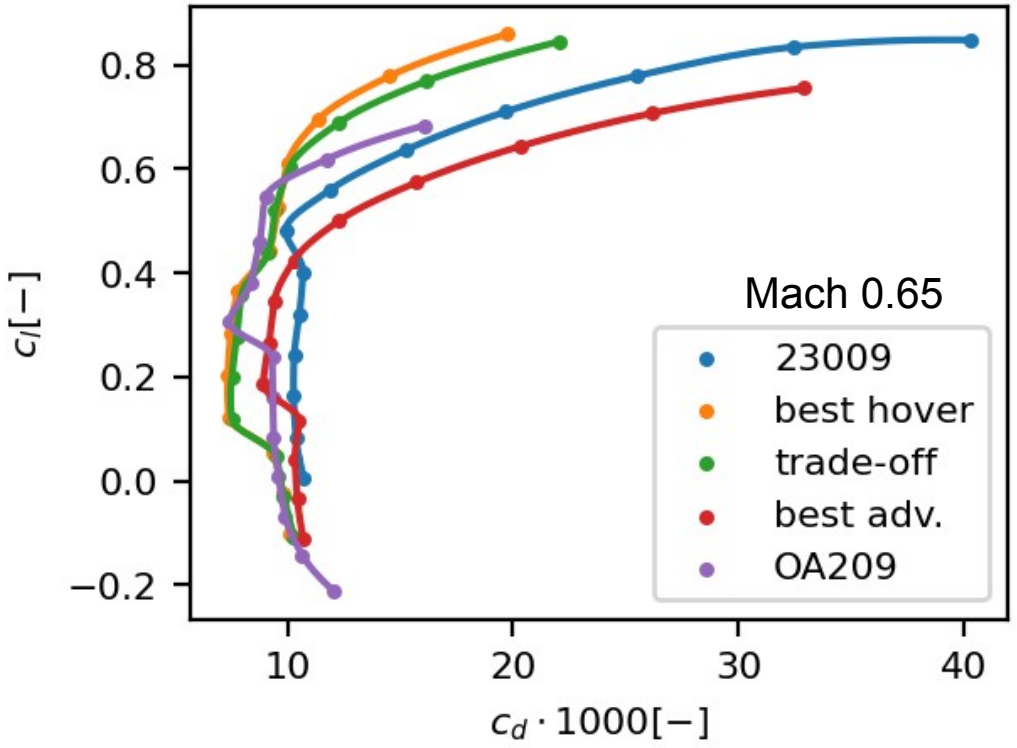

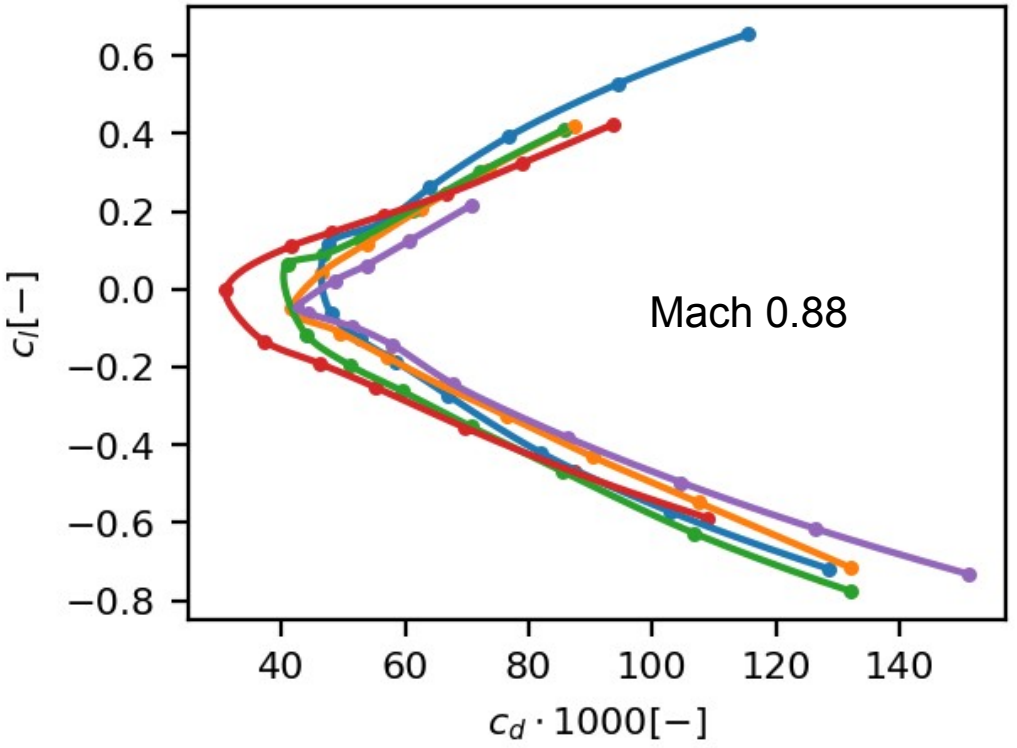

- The optimized airfoils show greater potential at lower lift coefficients in hover and superior over the NACA23009 and in a similar league as the OA209
- In forward flight, the best hover airfoil and the OA209 are superior in only one point, whereas the best adv. and trade-off airfoils can be considered robust designs as they improve over a larger range of lift coefficients.

Optimization Results: 9% outboard – pressure distributions @ mean c_l

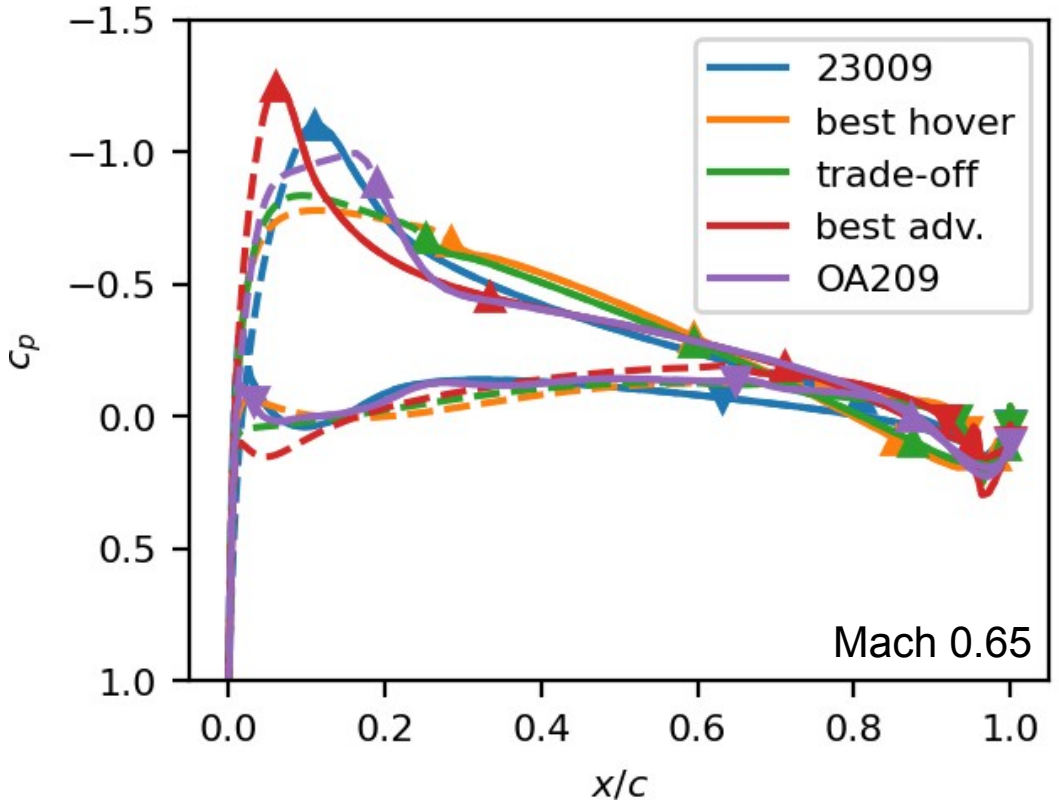

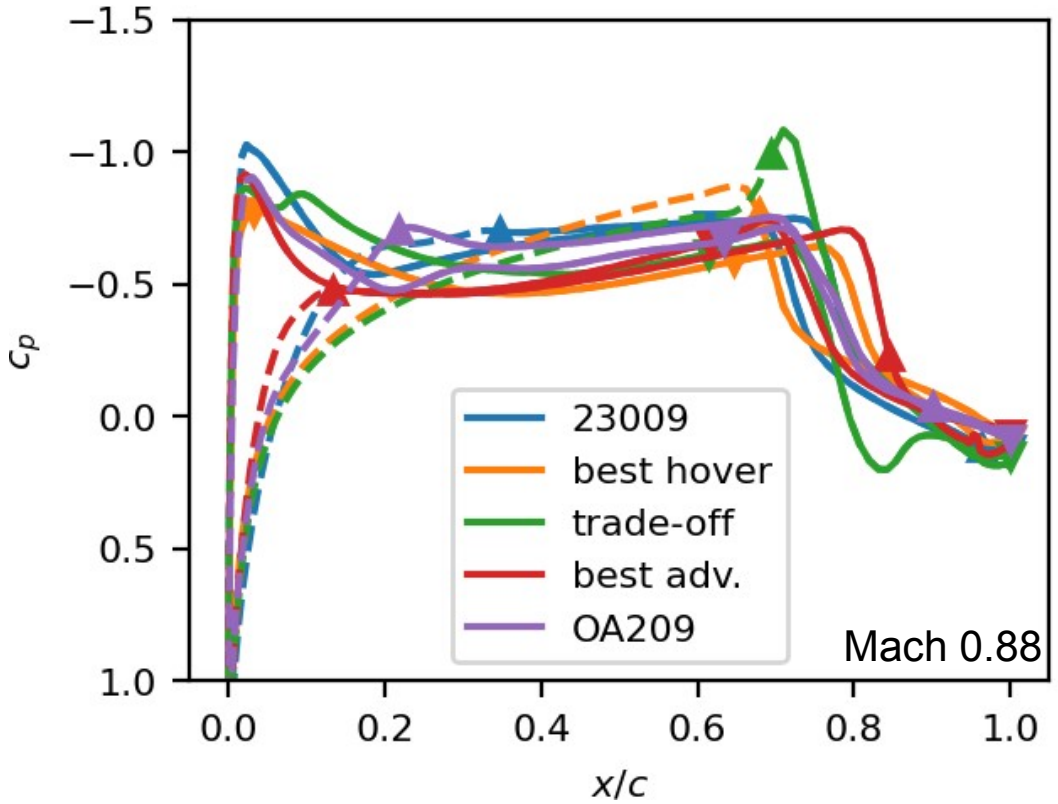

- All airfoils from the optimization show a longer laminar area on the pressure side in hover, yet the suction peak for the best adv. airfoil is more severe than it is for the NACA23009. The best adv. airfoil on the other hand shows the most delayed shock in the advancing side condition
- The trade-off airfoil shows a delay of the transition and shock of the suction side over the reference airfoil, yet the shock is stronger. The net effect is still in favor of this airfoil.

Verification of Rotor Design Gains

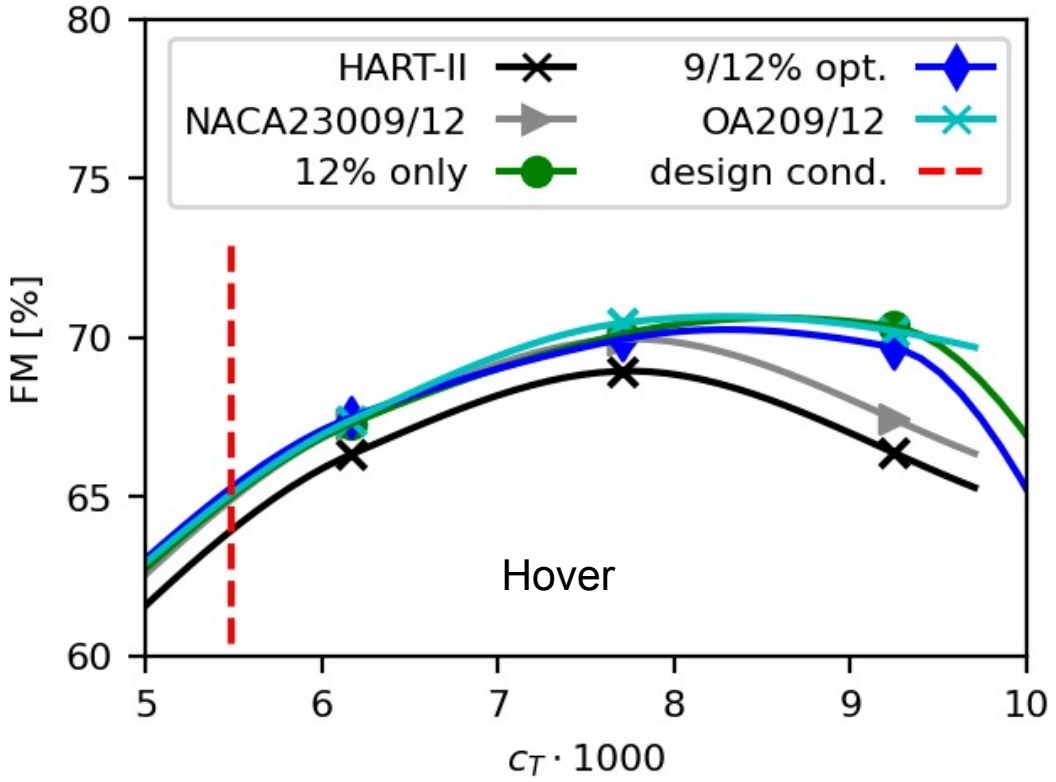

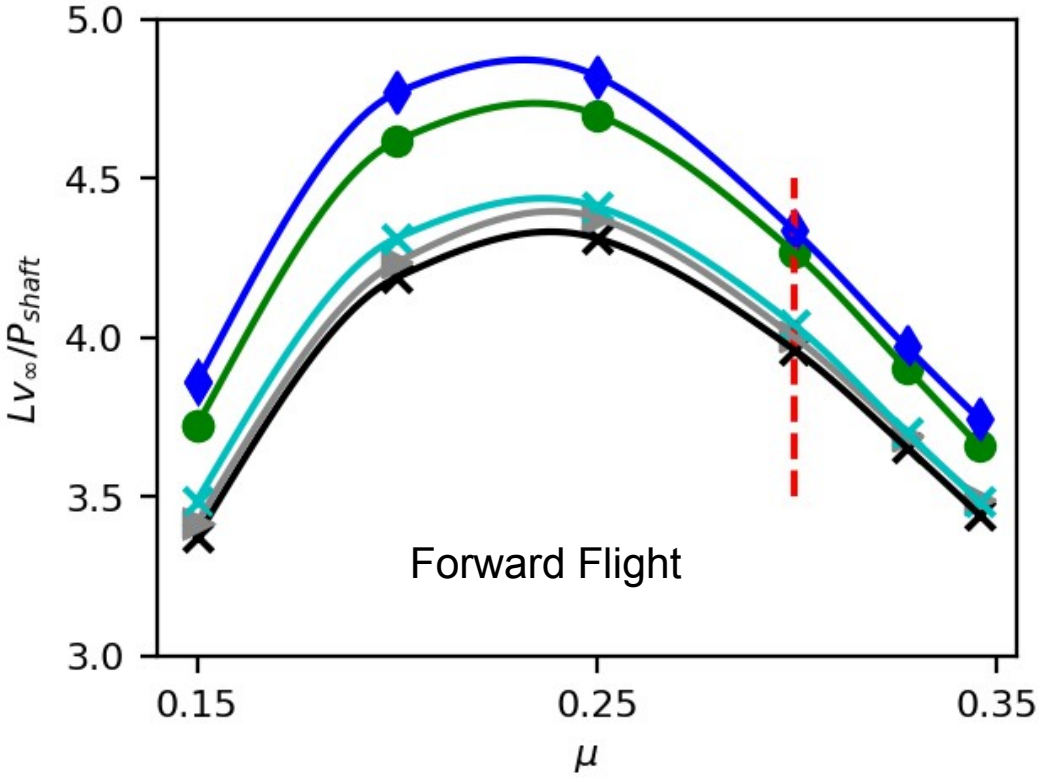

- Comparison of the new (trade-off) airfoils against the original HART II rotor, the HART II rotor with a NACA23009 at the tip and the OA212/OA209 airfoils. All airfoils aligned with their zero-lift angle of attack.
- A gain in all investigated flight conditions is found. The pure 12% optimized airfoil slightly better in hover then the 12% / 9% airfoil combination.
- Greatest gain in forward flight at intermediate advance ratios: reason is that the induced power is the smallest.

Summary

- Implemented an optimization framework taking into account renowned design guidelines. Efficient data generation for large range lift coefficient ranges using 3rd order accurate CFD simulations including transition prediction.

- The framework was validated and verified through the optimization of a publicly available rotor and known airfoil designs.

- Lessons learned:
  - Airfoil design is very constraint driven as Dadone [3] and Thibert and Gallot [4] already stated.
  - The airfoils by Thibert and Gallot (OA2xx) could be surpassed due the application of more robust design
  - 12% airfoils may be maintained over the blade span if maximum thrust in hover is important, otherwise to improve in forward flight, slimmer airfoils are crucial to alleviate wave drag.

- This work should be extended to include dynamic stall, investigate the effect on aero-acoustics and complement planform & twist optimization, i.e. a whole-some aerodynamic shape optimization.

Comment 9% Optimization

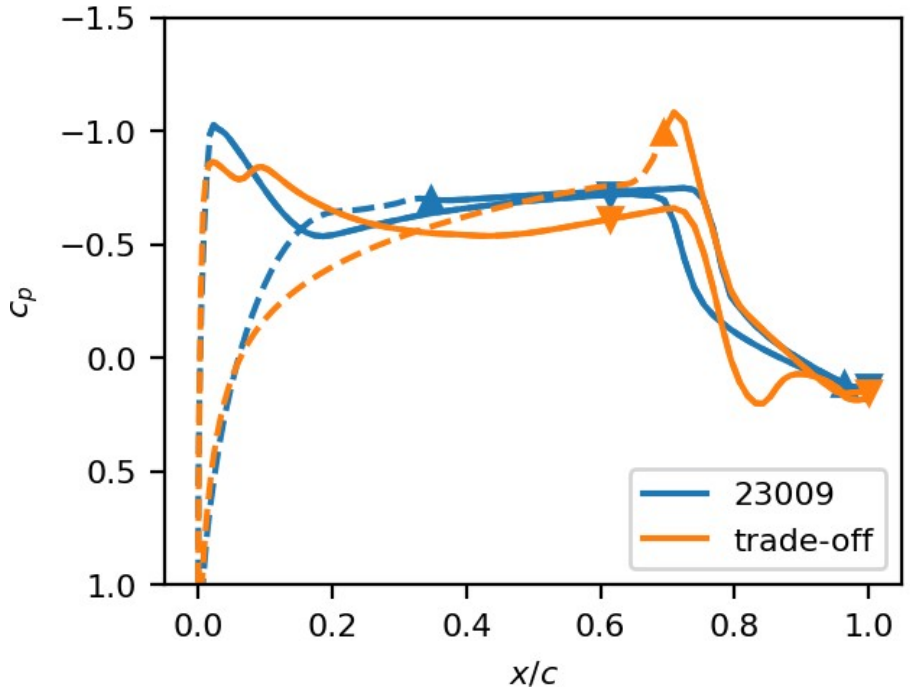

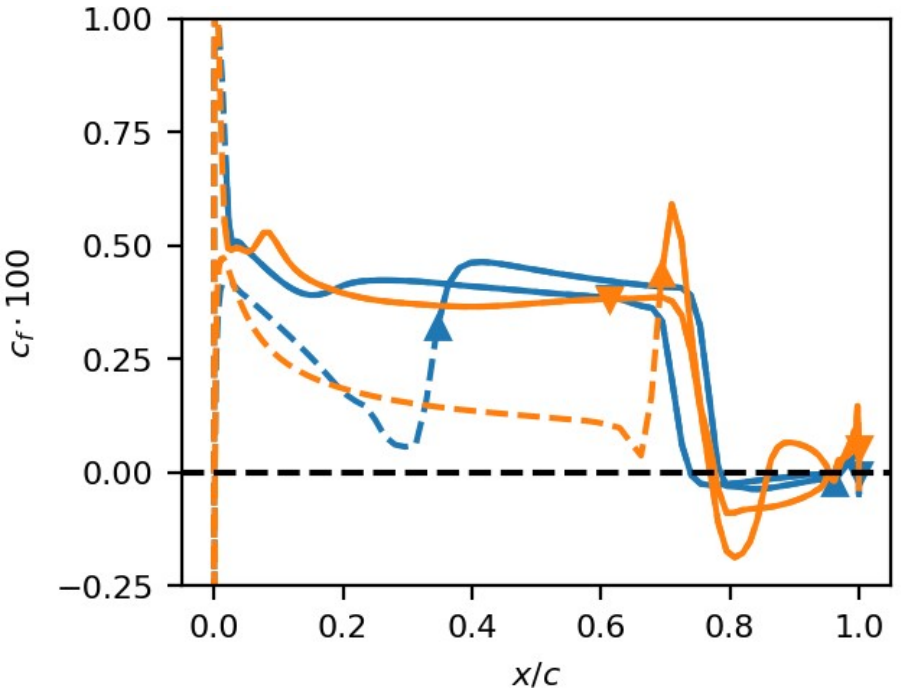

- “optical illusion” lets one assume a very large shock. It is still a large shock, but on top and bottom. The laminar region is still significantly larger than the reference airfoil.